J. Fluid Mech. (1979), *vol.* 90, *part* 2, *pp.* 305–314
Printed in Great Britain

High Reynolds number flows in exponential tubes of slow variation

By P. G. DANIELS AND P. M. EAGLES

Department of Mathematics, The City University,
St John Street, London EC1V 4PB

(Received 21 April 1978)

Axisymmetric high Reynolds number flows in tubes of slowly varying radius are shown to be governed to a first approximation and in suitable co-ordinates by a partial differential equation which, in a particular case, allows solutions independent of the streamwise co-ordinate. The solutions of the resulting ordinary differential equation give flows with inflexion points in the velocity profiles and reversed flow in some cases.

1. Introduction

In this paper we find a set of first approximations to axisymmetric solutions for incompressible flow in a tube of radius $H(Z)$, where $Z = \epsilon z$. Here z is the dimensionless co-ordinate in the axial direction and ϵ is a small parameter. The flow is mainly in the z direction so it is appropriate to introduce a Reynolds number $R = M/\nu L$, where M is the volumetric flow rate in that direction. The length L is the tube radius at some fixed station and ν is the kinematic viscosity.

In the case where $R = O(1)$ as $\epsilon \to 0$ the flow is a small perturbation of Poiseuille flow and has been treated by Blasius (1910), Manton (1971) and Tanner & Linnet (1965). The interest in the present work is to bring into play the nonlinear terms in the equations at the *first* approximation, and to this end we set $R\epsilon = \lambda$, where λ is a constant. As pointed out by Smith (1976), the first approximation to the flow then satisfies the boundary-layer equations, although the balance here is obtained in a manner quite different from that in conventional boundary-layer theory.

On using a Stokes stream function of the form $\psi = F_0(\eta, Z) + O(\epsilon^2)$, where $\eta = r/H(Z)$, we can find the partial differential equation for $F_0(\eta, Z)$. The observation is then made that this equation allows solutions independent of Z provided that $H(Z)$ takes the special form $H(Z) = \exp(aZ)$, where a is constant, which we choose to be positive.

The nonlinear ordinary differential equation for F_0 is displayed in (2.22) and that for the z velocity $G = \eta^{-1}dF_0/d\eta$ is shown in (2.26). The appropriate boundary-value problem for this velocity function has many interesting solutions, including velocity profiles with points of inflexion and reversed flow, and some with multiple maxima and minima. In this paper we have calculated numerically a selection of solutions which appear most likely to be attained experimentally and which merge smoothly with Poiseuille flow as $\lambda \to 0$. Some other solutions are also discussed.

It will appear that our expansion is valid for $\epsilon H \ll 1$ and this is certainly true for $Z < k|\log \epsilon|$, where k is a positive constant. The expansion, though formally valid for

$Z \to -\infty$, is of doubtful value for large negative values of Z because the local Reynolds number becomes very large and presumably the flow is unstable in many cases. It seems possible, however, that if we attach a tube of constant radius fairly smoothly to an exponential tube the flow described by our theory could be attained gradually as Z increases from negative values. Consideration of the transition from Poiseuille flow to our flows would be a complicated problem and will not be considered here.

The theory given here bears a certain resemblance to the theory of high Reynolds number flow in wedges of small angle. Specifically, if we consider channel walls of the form $y = \pm \epsilon x$ with $R\epsilon = \lambda$, where R is a Reynolds number, then the first approximation F to the stream function may be shown to satisfy the ordinary differential equation

$$F''' + 2\lambda F' F'' = 0. \tag{1.1}$$

Here $F = F(\eta)$ and $\eta = y/\epsilon x$. This, of course, is the first approximation in the limit $\epsilon \to 0$ with λ fixed to the *exact* Jeffery–Hamel solutions for flow in a wedge with arbitrary ϵ and R.

However, in the case of a cone there is no simple exact solution, therefore the flows described here are a first approximation to a more complicated situation. A major difference is that as x is varied the local Reynolds number and local divergence angle remain constant in the wedge, but as z is varied in the tube the local values of R and the divergence angle change. This is the basic reason for the restriction $\epsilon H \ll 1$ required in our theory. This point will be discussed more fully later.

In view of Fraenkel's (1962, 1963) theory of flow in channels of small wall curvature, using the Jeffery–Hamel solutions as a first approximation, it is natural to ask whether a similar approach would work for tubes which behave locally like tubes of radius $\exp(aZ)$. This question is currently under investigation and results will be reported at a later date.

Another question of interest is that of the stability of the flows obtained. We know that Poiseuille flow is stable to infinitesimal disturbances (see, for example, Davey & Nguyen 1971). As $\gamma = \lambda a$ increases in (2.26) the flows change from Poiseuille flow to flows with points of inflexion in the velocity profile. It seems likely that these flows will become unstable at some value of γ. The investigation of this would require computation of the stability problem for high Reynolds numbers, which is not an easy task.

2. Expansion for flow in tubes of slowly varying radius

Let (r^*, θ, z^*) be cylindrical polar co-ordinates and let $\psi^*(r^*, z^*)$ be a Stokes stream function such that

$$u^* = -r^{*-1}\partial\psi^*/\partial z^*, \quad v^* = r^{*-1}\partial\psi^*/\partial r^*. \tag{2.1}$$

are the fluid velocities in the radial and axial directions respectively. We wish to consider flow in tubes with rigid boundaries given by

$$r^* = g^*(z^*). \tag{2.2}$$

We define the constant volumetric flow rate M to be

$$M = \int_0^{2\pi}\int_0^{g^*} v^* r^* dr^* d\theta = 2\pi[\psi^*(g^*, z^*) - \psi^*(0, z^*)]. \tag{2.3}$$

Taking ψ^* to be zero on the axis $r^* = 0$ this requires

$$\psi^* = M/2\pi \quad \text{on} \quad r^* = g^*. \tag{2.4}$$

The dimensionless co-ordinates and stream function are defined by

$$r = r^*/L, \quad z = z^*/L, \quad \psi = \psi^*/M, \tag{2.5}$$

where L is the tube radius at $z = 0$. The radius of the tube is now given by

$$r = Q(z), \tag{2.6}$$

where $Q(z) = g^*(z^*)/L$ and we note that $Q(0) = 1$. The equation for ψ is

$$\frac{1}{r^2}\left(\frac{\partial\psi}{\partial r}\frac{\partial}{\partial z} - \frac{\partial\psi}{\partial z}\frac{\partial}{\partial r}\right)D^2\psi + \frac{1}{r^3}\left(2\frac{\partial\psi}{\partial z}\frac{\partial^2\psi}{\partial z^2} + 3\frac{\partial\psi}{\partial z}\frac{\partial^2\psi}{\partial r^2} - \frac{\partial\psi}{\partial r}\frac{\partial^2\psi}{\partial r\,\partial z}\right) - \frac{3}{r^4}\left(\frac{\partial\psi}{\partial z}\frac{\partial\psi}{\partial r}\right)$$
$$= \frac{1}{R}\left\{\frac{1}{r}D^4\psi - \frac{2}{r^2}\left(\frac{\partial^3\psi}{\partial r\,\partial z^2} + \frac{\partial^3\psi}{\partial r^3}\right) + \frac{3}{r^3}\frac{\partial^2\psi}{\partial r^2} - \frac{3}{r^4}\frac{\partial\psi}{\partial r}\right\}, \tag{2.7}$$

where
$$D^2 = \partial^2/\partial r^2 + \partial^2/\partial z^2 \tag{2.8}$$

and R is the Reynolds number

$$R = M/\nu L, \tag{2.9}$$

ν being the kinematic viscosity.

We prefer the above more explicit form to the version quoted by, for example, Goldstein (1943, p. 115), and it should be noted that our D^2 is different from Goldstein's and that our ψ is of opposite sign. The boundary conditions are

$$\left.\begin{aligned} &\text{(i)} \quad \psi = O(r^2) \quad \text{as} \quad r \to 0, \\ &\text{(ii)} \quad \partial\psi/\partial r = 0 \quad \text{when} \quad r = Q(z), \\ &\text{(iii)} \quad \psi = 1/2\pi \quad \text{when} \quad r = Q(z), \end{aligned}\right\} \tag{2.10}$$

where from (2.1) we see that (i) ensures that the fluid velocity is finite at the centre of the tube while (ii) and (iii) ensure that it is zero on the tube wall $r = Q(z)$. Further conditions are needed for a complete specification of the problem.

We now specialize to the particular case in which the walls are slowly varying in the z direction, i.e. we assume that the tube walls are given by

$$r = H(Z), \tag{2.11}$$

where $Z = \epsilon z$ and ϵ is small. Assuming then a corresponding Stokes stream function

$$\psi = \hat{\psi}(r, Z), \tag{2.12}$$

we see that since $\partial/\partial z$ in (2.7) becomes $\epsilon\partial/\partial Z$ the dominant terms on the left-hand side are of order ϵ while those on the right-hand side are $1/R$ times terms of order one. We are thus led to consider flows in which

$$\epsilon R = \lambda. \tag{2.13}$$

The dominant terms on each side are then of order ϵ, while the next-order terms occurring in the equation for $\hat{\psi}$ are of order ϵ^3.

Since the boundary conditions do not contain ϵ an expansion

$$\hat{\psi} = \hat{\psi}_0(r, Z) + \epsilon^2\hat{\psi}_2(r, Z) + \ldots \tag{2.14}$$

is appropriate. It is also useful to introduce the co-ordinate

$$\eta = r/H(Z). \tag{2.15}$$

Then $\eta = 1$ is the wall of the tube. We set

$$\psi = F_0(\eta, Z) + \epsilon^2 F_2(\eta, Z) + \ldots, \tag{2.16}$$

and using (2.13) and the transformations

$$\frac{\partial}{\partial z} \to -\epsilon\eta \frac{H'(Z)}{H(Z)} \frac{\partial}{\partial \eta} + \epsilon \frac{\partial}{\partial Z}, \quad \frac{\partial}{\partial r} \to \frac{1}{H} \frac{\partial}{\partial \eta} \tag{2.17}$$

in the stream-function equation (2.7), we find that the partial differential equation for F_0 is

$$\mathscr{L}(F_0) = \lambda \left[\frac{4H'(Z)}{H(Z)} \left(\frac{1}{\eta^2} \left\{ \frac{\partial F_0}{\partial \eta} \right\}^2 - \frac{1}{\eta} \frac{\partial F_0}{\partial \eta} \frac{\partial^2 F_0}{\partial \eta^2} \right) + \frac{\partial F_0}{\partial \eta} \left(\frac{1}{\eta} \frac{\partial^3 F_0}{\partial \eta^2 \partial Z} - \frac{1}{\eta^2} \frac{\partial^2 F_0}{\partial \eta \partial Z} \right) + \frac{\partial F_0}{\partial Z} \left(-\frac{1}{\eta} \frac{\partial^3 F_0}{\partial \eta^3} + \frac{3}{\eta^2} \frac{\partial^2 F_0}{\partial \eta^2} - \frac{3}{\eta^3} \frac{\partial F_0}{\partial \eta} \right) \right], \tag{2.18}$$

where

$$\mathscr{L} \equiv \frac{\partial^4}{\partial \eta^4} - \frac{2}{\eta} \frac{\partial^3}{\partial \eta^3} + \frac{3}{\eta^2} \frac{\partial^2}{\partial \eta^2} - \frac{3}{\eta^3} \frac{\partial}{\partial \eta}. \tag{2.19}$$

We now make the crucial observation that if $H'(Z) = aH(Z)$ then (2.18) allows a solution which is independent of Z, i.e. a function of η only. Thus setting

$$H(Z) = \exp(aZ), \tag{2.20}$$

where a is constant, which we choose to be positive, and setting

$$\psi = F_0(\eta) + \epsilon^2 F_2(\eta, Z) + \ldots, \tag{2.21}$$

we find that the ordinary differential equation for F_0 is

$$F_0^{\mathrm{iv}} - \frac{2}{\eta} F_0''' + \frac{3}{\eta^2} F_0'' - \frac{3}{\eta^3} F_0' + 4\lambda a \left(\frac{F_0' F_0''}{\eta} - \frac{F_0'^2}{\eta^2} \right) = 0. \tag{2.22}$$

The boundary conditions corresponding to (2.10) are

$$F_0 = O(\eta^2) \quad \text{as} \quad \eta \to 0, \quad F_0'(1) = 0, \quad F_0(1) = 1/2\pi. \tag{2.23}$$

Equation (2.22) is singular at $\eta = 0$ and allows a series solution starting with

$$(a_0 + a_2\eta^2 + a_4\eta^4 + \ldots) + b_0(\eta^2 \log \eta + \ldots), \tag{2.24}$$

where the constants a_0, a_2, a_4 and b_0 are arbitrary as far as the differential equation is concerned. From (2.23) we require $a_0 = 0$ and $b_0 = 0$, the latter ensuring that $F_0(\eta)$ is regular at $\eta = 0$.

In terms of the velocity function $G(\eta)$ defined as

$$G(\eta) = \eta^{-1} dF_0/d\eta \tag{2.25}$$

the differential equation becomes

$$G''' + \eta^{-1} G'' - \eta^{-2} G' + 4\gamma GG' = 0, \tag{2.26}$$

where $\gamma = \lambda a$. The boundary conditions may be expressed as

$$\left.\begin{aligned} &G(\eta) \text{ regular at } \eta = 0, \\ &\int_0^1 \eta G(\eta)\, d\eta = 1/2\pi, \quad G(1) = 0. \end{aligned}\right\} \tag{2.27}$$

In §3 we discuss some solutions of this nonlinear boundary-value problem. It turns out that there are some interesting solutions with points of inflexion and reversed flow, and also some with several maxima and minima. It should perhaps be pointed out that $\gamma > 0$ represents flow with a net volumetric flow rate which is positive, i.e. flow in a divergent tube, while $\gamma < 0$ represents net flow into a convergent tube. The case $\gamma = 0$ can be interpreted as $R = 0$, with solution $G = 0$, or as $a = 0$, R arbitrary, with a Poiseuille-flow solution.

We now consider briefly the solution for the next perturbation function $F_2(\eta, Z)$. We find that $F_2(\eta, Z)$ may be expressed in the form

$$F_2(\eta, Z) = a^2 \exp(2aZ)\, \hat{F}_2(\eta). \tag{2.28}$$

Substituting (2.21) with (2.28) into (2.7) and equating coefficients of ϵ^2 yields a fourth-order linear ordinary differential equation for $\hat{F}_2$ containing only γ as a parameter. This may in principle be solved subject to the boundary conditions

$$\left.\begin{aligned} \hat{F}_2 &= O(\eta^2) \quad \text{as} \quad \eta \to 0, \\ \hat{F}_2(1) &= \hat{F}_2'(1) = 0. \end{aligned}\right\} \tag{2.29}$$

It seems that for validity of the expansion in an asymptotic sense as $\epsilon \to 0$ we need

$$\epsilon \exp(aZ) \ll 1. \tag{2.30}$$

This is satisfied for any negative value of Z and for positive values of Z such that $Z \ll |\log \epsilon|$, i.e. such that $z \ll \epsilon^{-1}|\log \epsilon|$.

For large negative values of Z, e.g. $Z \sim -\epsilon^{-n}$, the error in using only the first term appears to be transcendentally small. But the local Reynolds number

$$R_L = M/\nu LH = R \exp(-aZ) \tag{2.31}$$

is then transcendentally large, and the flow may be unstable.

For large positive values of Z (formally $Z \gg |\log \epsilon|$) the expansion fails. This is to be expected because

$$dH/dz = a\epsilon \exp(aZ) \tag{2.32}$$

is then no longer small, i.e. the local divergence angle of the walls is no longer small. The product of the local Reynolds number and the local divergence angle remains constant, but the basis for the approximation is destroyed.

The first approximation appears to have error of order ϵ^2 if $-K_1 < Z < K_2$, where K_1 and K_2 are positive constants, i.e. provided that $-K_1/\epsilon < z < K_2/\epsilon$. This would probably be a useful range for application of the theory with reasonable values of ϵ and with K_1 and K_2 chosen to be numerically of order 1.

3. Solutions for $G(\eta)$

We now consider solutions for the velocity function $G(\eta)$, which must satisfy the equation (2.26) and boundary conditions (2.27). One integration of (2.26) yields

$$G'' + \eta^{-1}G' + 2\gamma G^2 = C, \tag{3.1}$$

where C is a constant. The first of the boundary conditions (2.27) excludes the possibility of a term of order $\log \eta$ in the expansion of G as $\eta \to 0$, which then has the form

$$G \sim 2a_2 + 4a_4\eta^2 \quad (\eta \to 0), \tag{3.2}$$

where a_2 and a_4 are the coefficients in (2.24). Also $C = 8(2a_4 + \gamma a_2^2)$. Negative and positive values of the parameter γ correspond to flow in converging and diverging tubes respectively while the particular case $\gamma = 0$ corresponds to Poiseuille flow in a straight-walled tube.

Solutions for G were computed for a range of values of γ using two alternative numerical schemes. In the first the system

$$\bar{G}'' + \bar{\eta}^{-1}\bar{G}' + d_1\bar{G}^2 = d_2, \quad \bar{G}(0) = 1, \quad \bar{G}'(0) = 0, \tag{3.3}$$

for $\bar{G}(\bar{\eta})$ was solved using a second-order-accurate finite-difference scheme in which d_1 and d_2 are given specified values and the solution then computed forwards from $\bar{\eta} = 0$ until $\bar{G} = 0$ at $\bar{\eta} = c_1$ (say). Then c_2 is defined by

$$c_2 = \int_0^{c_1} \bar{\eta}\bar{G}\, d\bar{\eta}$$

and the required solution of (2.26) and (2.27) is

$$G(\eta) = (c_1^2/2\pi c_2)\,\bar{G}(\bar{\eta}), \quad \eta = c_1^{-1}\bar{\eta}, \quad \gamma = \pi c_2 d_1. \tag{3.4}$$

In this way solutions are obtained by just one forward integration from $\eta = 0$ and the extension to solutions with more than one zero of G is straightforward. The disadvantage of this method is that the value of γ cannot be prescribed at the outset, being determined by (3.4). More accurate solutions were obtained for prescribed γ by applying a fourth-order Runge–Kutta scheme to the system (2.26) and (2.27). The starting values a_2 and a_4 were set and adjusted after forward integration to $\eta = 1$ using linear interpolation until the second and third conditions in (2.27) were satisfied. As a check on accuracy the series solution was found up to η^8 and used instead of the first Runge–Kutta step. As in the first scheme, integration from a finite value of G automatically excludes the possibility of logarithmic behaviour at $\eta = 0$.

Figure 1 shows the scaled non-dimensional skin friction $-G'(1)$ at the wall as a function of γ. There are multiple solutions for both positive and negative values of γ, although it seems likely that the solutions on branch 1, which we believe to be accurate to within 0·1 % and which are shown in detail in figure 1 (*b*), are the only ones which are physically realistic. Velocity profiles associated with this branch are shown in figure 2. We see that as $\gamma \to -\infty$ the profile is virtually uniform across the tube; the predominant balance in (3.1) is

$$G \sim (-C/2|\gamma|)^{\frac{1}{2}} \quad (-\gamma \gg 1) \tag{3.5}$$

and the flux condition requires that away from the wall

$$C = -2|\gamma|\pi^{-2}, \quad G \sim \pi^{-1}. \tag{3.6}$$

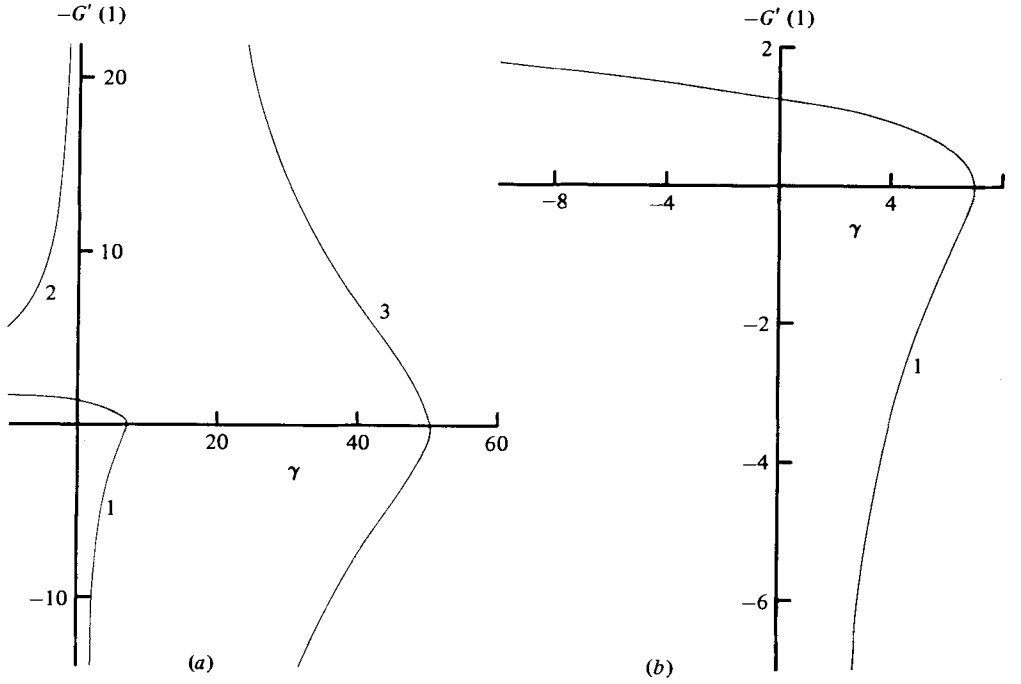

FIGURE 1. Some branches of the solution of (2.26) and (2.27).

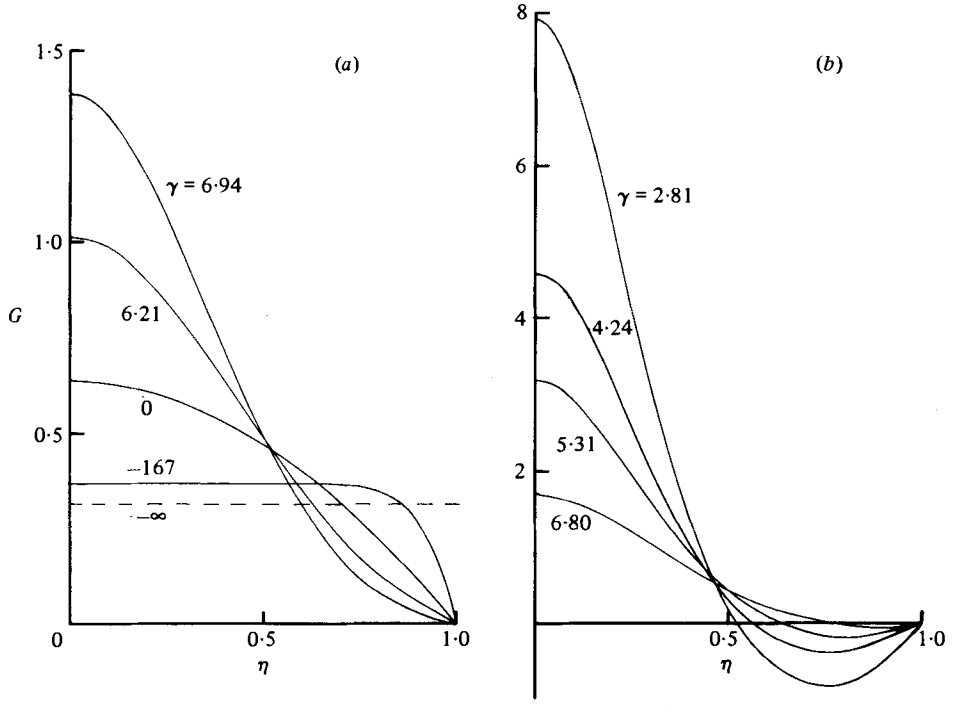

FIGURE 2. Velocity profiles on branch 1 for various values of γ.

A boundary layer must adjust the velocity to zero at the wall $\eta = 1$. We therefore write $\eta = 1-(\pi/|\gamma|^{\frac{1}{2}})\,\eta_1$ and consider the region where $\eta_1 = O(1)$. Here the solution which matches with (3.6) as $\eta_1 \to \infty$ is

$$G = \pi^{-1}(3\tanh^2(\eta_1+d)-2)+O(|\gamma|^{-\frac{1}{2}}) \quad (-\gamma \gg 1) \tag{3.7}$$

and the wall condition at $\eta_1 = 0$ is also satisfied provided that

$$d = \pm\tanh^{-1}(\tfrac{2}{3})^{\frac{1}{2}} \simeq \pm 1{\cdot}146. \tag{3.8}$$

The solution with $d > 0$ represents a monotonic increase in velocity from zero at the wall to the mainstream value (3.6) and is the asymptotic solution on branch 1 as $\gamma \to -\infty$. The solution to this order is essentially that obtained in the boundary layer between converging plane walls. The solution with $d < 0$ contains a reverse flow region in the boundary layer at the wall and corresponds to a different branch of the solution, which is discussed below.

On branch 1 the velocity at the centre of the tube increases as γ is increased through negative values and at $\gamma = 0$ we have the parabolic Poiseuille profile

$$G = 2\pi^{-1}(1-\eta^2), \quad -G'(1) = 4\pi^{-1}. \tag{3.9}$$

A further increase in γ results in the development of an inflexion point in the profile at $\gamma \simeq 4{\cdot}9$, $\eta \simeq 0{\cdot}5$ and eventually separation occurs at the tube wall (i.e. $G'(1) = 0$) when $\gamma = \gamma_0 \simeq 6{\cdot}944$.

Our numerical results suggested that the solution for G as a function of γ is singular at the point of separation and this is confirmed analytically as follows. We suppose that γ_n ($n = 0, 1, 2, \ldots$) is a value of γ at which $G'(1) = 0$ and expand G in the form

$$G = G_0(\eta)+(\gamma_n-\gamma)^{\frac{1}{2}}G_1(\eta)+(\gamma_n-\gamma)\,G_2(\eta)+\ldots \tag{3.10}$$

as $\gamma \to \gamma_n$. Substitution into (3.1) shows that the functions G_0, G_1 and G_2 must satisfy

$$G_0''+\frac{1}{\eta}G_0'+2\gamma_n G_0^2 = C_0, \quad G_0(1) = 0, \quad \int_0^1 \eta G_0\,d\eta = \frac{1}{2\pi}, \tag{3.11}$$

$$G_1''+\frac{1}{\eta}G_1'+4\gamma_n G_0 G_1 = C_1, \quad G_1(1) = 0, \quad \int_0^1 \eta G_1\,d\eta = 0, \tag{3.12}$$

$$G_2''+\frac{1}{\eta}G_2'+4\gamma_n G_0 G_2 = C_2+2G_0^2-2\gamma_n G_1^2, \quad G_2(1) = 0, \quad \int_0^1 \eta G_2\,d\eta = 0 \tag{3.13}$$

in addition to the requirements of regularity at $\eta = 0$. Since $G_0'(1) = 0$ the required solution for G_1 may be found as

$$G_1 = A(G_0+\tfrac{1}{2}\eta G_0'), \tag{3.14}$$

where A is an arbitrary constant. However, a consistent solution for G_2 may be found only if

$$A^2 = \frac{16\int_0^1 \eta G_0^3\,d\eta}{\gamma_n\int_0^1 \eta^3(G_0')^2\,(6G_0+\eta G_0')\,d\eta}, \tag{3.15}$$

a result obtained by multiplication of (3.12) by ηG_2 and (3.13) by ηG_1, subtraction and integration from $\eta = 0$ to $\eta = 1$. Our numerical results suggest that this expression for A^2 is always positive, both integrals involved being positive for $n = 0$ (branch

1). Thus having found G_0 (in theory) from (3.11), A is determined and the solution for G_1 complete. The reason for the singularity at γ_n is now evident: a regular expansion about this point (i.e. with $G_1 = 0$) would imply that the solution (3.14) is one component of the solution for G_2. The full solution for G_2 would then contain the arbitrary constants A and C_2, one further constant, B, say, and the particular integral corresponding to the term $2G_0^2$ on the right-hand side. In general the three constants A, B and C_2 would be chosen to satisfy the two conditions in (3.13) and the requirement of regularity at $\eta = 0$. However with $G_0'(1) = 0$ the value of A has no influence upon these conditions and the remaining two constants B and C_2 cannot be chosen to satisfy the three boundary conditions. Introduction of the term of order $(\gamma_n - \gamma)^{\frac{1}{2}}$ in (3.10) provides the extra term $-2\gamma_n G_1^2$ on the right-hand side of (3.13) which allows this situation to be avoided.

Beyond the point of separation at γ_0, the branch 1 profiles contain reverse flow regions at the wall which increase in size and strength as $\gamma \to 0+$. Here the solution of (3.1) has the form

$$G = \gamma^{-1}\tilde{G}(\eta) + \ldots \quad (\gamma \to 0), \tag{3.16}$$

where $\tilde{G}$ must be found as a solution of the nonlinear eigenvalue problem

$$\tilde{G}'' + \frac{1}{\eta}\tilde{G}' + 2\tilde{G}^2 = \tilde{C}, \quad \tilde{G}(1) = 0, \quad \int_0^1 \eta \tilde{G}\, d\eta = 0, \quad \tilde{G}(0) \text{ finite}, \tag{3.17}$$

where $\tilde{C}$ is an arbitrary constant to be determined.

We envisage that there will be a doubly infinite set of solutions of (3.17), $\tilde{G} = \tilde{G}_m^{\pm}$ ($m = 1, 2, \ldots$) say (where $\pm$ represents solutions with $\tilde{G}(0) \gtrless 0$), and that the solution $\tilde{G}_m$ will have m zeros in the region $0 \leqslant \eta < 1$. The eigenfunction $\tilde{G}_1^+$ describes both the solution on branch 1 as $\gamma \to 0+$ (see figure 2*b*) and the solution on branch 2 (see figure 1*a*) as $\gamma \to 0-$. The latter has a region of reverse flow at the centre of the tube and forward flow adjacent to the walls (see figure 3). On branch 3 (also shown in figure 1*a*) the solution starts in the form (3.16) with $\tilde{G} = \tilde{G}_1^-$ (reverse flow at the centre) at the upper extreme, separation occurs at the parabolic vertex at

$$\gamma = \gamma_1 \simeq 50{\cdot}4,$$

below the γ axis an additional region of reverse flow appears at the wall, and as $\gamma \to 0+$ the solution has the form (3.16) with $\tilde{G} = \tilde{G}_2$.

In the region $\gamma < 0$ the branch 1 solution develops into the profile (3.6), (3.7) as $\gamma \to -\infty$, while the branch which takes the form (3.16) with $\tilde{G} = \tilde{G}_1^-$ as $\gamma \to 0-$ develops into the same uniform profile (3.6) as $\gamma \to -\infty$ but with the minus sign for d in (3.8), representing a reverse flow region in the boundary layer at the wall. The remaining branches in $\gamma < 0$ contain increasing numbers of reverse flow regions and it seems likely that as $\gamma \to -\infty$ these will be compressed into shear layers of thickness $O(|\gamma|^{-\frac{1}{2}})$, centred at stations $\eta = \eta_0$ in the fluid, where the velocity profile is

$$G \sim \pi^{-1}\{3\tanh^2(\pi^{-\frac{1}{2}}|\gamma|^{\frac{1}{2}}(\eta - \eta_0) - 2)\}. \tag{3.18}$$

These layers will separate regions of forward flow where $G \sim \pi^{-1}$.

We expect that all the branches with reverse flow are unstable and although we have not yet carried out a detailed stability analysis, we note that the point $\gamma = \gamma_0$ on branch 1 is a point of marginal stability to disturbances which are simply functions

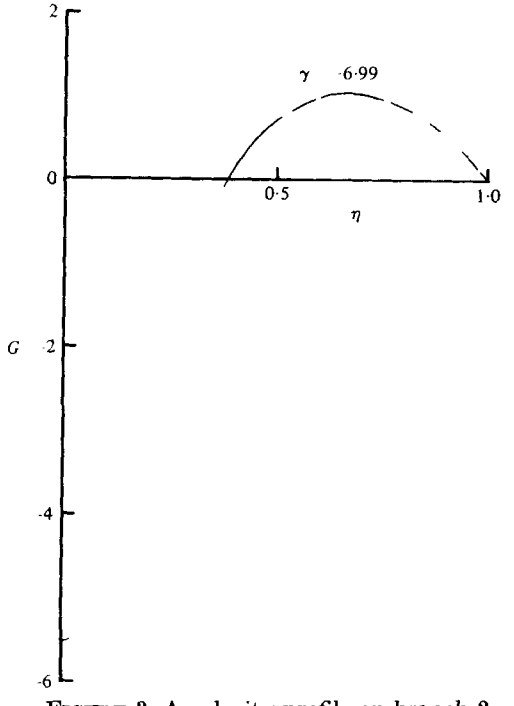

FIGURE 3. A velocity profile on branch 2.

of η. This is because a solution of the form (3.14) may be regarded as the leading eigenfunction of the disturbance with zero growth rate. It seems probable that only the solutions on branch 1 above the vertex are stable to such disturbances although the appearance of an inflexion point in the velocity profile suggests that more general disturbances may lead to instability at a lower value of γ.

REFERENCES

BLASIUS, H. 1910 *Z. Math. Phys.* **58**, 225.

DAVEY, A. & NGUYEN, H. P. F. 1971 *J. Fluid Mech.* **45**, 191.

FRAENKEL, L. E. 1962 *Proc. Roy. Soc.* A **267**, 119.

FRAENKEL, L. E. 1963 *Proc. Roy. Soc.* A **272**, 406.

GOLDSTEIN, S. (ed.) 1943 *Modern Developments in Fluid Dynamics*. Oxford University Press.

MANTON, M. J. 1971 *J. Fluid Mech.* **49**, 451.

SMITH, F. T. 1976 *Quart. J. Mech. Appl. Math.* **29**, 344.

TANNER, R. & LINNET, I. 1965 *2nd Austral. Conf. Hydraul. Fluid Mech. Rep.* A **159**.